Electronic Supplementary Material (ESI) for Lab on a Chip.

SUPPLEMENTARY INFORMATION

Calibration

Before a chip is used, a calibration experiment is first run to determine the fluidic resistance values referred to in the Theory section.

For the calibration, the middle inlet reservoir is first loaded with the same fluorescent dye used throughout. Then, the two side reservoirs are loaded with buffer and 60 mBar pressure is applied equally to all reservoirs. The pressure applied to the middle inlet reservoir is then reduced until the middle stream is seen to reduce to nothing. At this point the flow is stagnated in the middle channel so the pressure at the junction must be equal to the pressure applied to the middle channel. Under these conditions, if the flowrate through the main channel can be determined then its resistance (R_4) can be calculated trivially via:

S1-1: $$R_4 = \frac{P_j - P_o}{Q}$$

Where P_j is the pressure at the junction, P_o is atmospheric pressure and Q is the flow rate in the main channel.

To measure the flowrate we introduce a short plug of dye into the channel before returning to stagnation conditions. This is achieved by sending a quick (~30 second) pulse of high pressure (80 mBar) to the middle reservoir before returning it to the stagnation pressure. This results in a wide plug of dye entering the device as shown in Figure SI-1. Once the pressure returns to stagnation the velocity of the plug through the chip is measured to determine the flowrate and R_4 is calculated.

This test also tells us the combined effect of the side inlet resistances R_1 and R_3 and we can write

S1-2 $$R_1 + R_3 = \frac{P_{in} - P_j}{Q}$$

Where P_{in} is the pressure at the inlets.

To make use of this, the ratio of R_1 to R_3 is determined by observing the percentage of the channel taken up by each inlet's stream during the stagnation part of the calibration. Consider the equation for flow rate through an arbitrary inlet channel:

S1-3 $$Q_n = \frac{P_{in} - P_j}{R_n}$$

Where Q_n is the flow through the nth inlet, and R_n is the resistance of the nth inlet channel. The ratio of Q_1 to Q_3 can then be expressed as:

SI-4 $$\frac{Q_1}{Q_2} = \frac{R_2}{R_1}$$

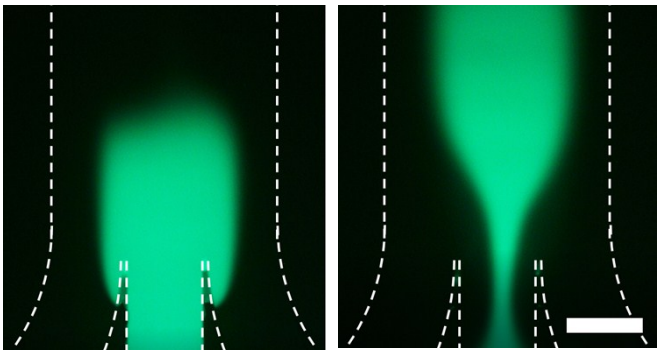

Figure SI-1: Sending a plug of dye through the chip for calibration of inlet pressures. (left) The plug of dye moving through the channel with inlet pressures of 60 mBar 80 mBar and 60 mBar from left to right. The velocity of the plug during this part of the test is used to determine the resistance of the central inlet after all other resistances are determined. (right) The plug 40 seconds later after switching the central inlet back to the stagnation pressure. After the flow in the central inlet has fully stagnated, the velocity of the plug is used to determine the side inlet resistances and the resistance of the main channel.

Which is directly measurable as the ratio of the stream widths and via equation SI-2 can be used to determine R_1 and R_3 as:

$$R_1 = \left(1 + \frac{Q_3}{Q_1}\right)\frac{P_{in} - P_j}{Q} \quad \text{SI-5}$$

$$R_3 = \left(1 + \frac{Q_1}{Q_3}\right)\frac{P_{in} - P_j}{Q} \quad \text{SI-6}$$

Finally the resistance of the central inlet must be determined. We do this using the measured flowrate during the pulse and equation SI-3 for the central inlet. Notice that all the variables are determined except for the resistance of central inlet channel R_2 which can thus be solved for easily.

After these simple calculations, all resistances in the system are known and equation 4 may be used to determine the flowrate through any or all inlet channels for a given set of inlet pressures.

Note that this calibration chiefly corrects for error during collagen filling of the of the inlet channels. The devices are filled from the center inlet and inevitably one inlet ends up slightly more filled than the other. This results in an average deviation of resistance from inlet to inlet of 8% (with a maximum of 12%) in our case.

Diffusivity

The diffusivity of the labeled dextran was empirically determined in our gel using the 2D gel filled chips. For this experiment the flows were configured such that the right half of the channel was initially filled with the dye. The boundary was initially kept sharp by using a relatively high flow velocity (60 µm/s) then allowed to freely diffuse by abruptly stopping the flow. As the dye diffused we measure the profile at two time points and fit the single sided version of equation 7 (shown here as SI-6) for D.

$$c_t(x,t) = c_o \mathrm{erf}\left(\frac{x}{\sqrt{4Dt}}\right) \quad \text{SI-6}$$

Width Control

Figure SI-2 compares the measured width of the concentration profile with the width predicted by equation 8 plotted against the target stream width instead of the target profile width. Notice that the predicted curve is consistently below the measured data for target widths greater than 150 microns. Note that while this is unexpected and interesting, it does not seem to detrimentally affect the controllability of the chip and could be calibrated for in future work.

We propose two possible explanations of the observed difference between theory and model, though both would require further work to validate.

First, the difference between data and theory may come from fabrication defects in the chips. Thin negative features were not successfully reproduced during lithography

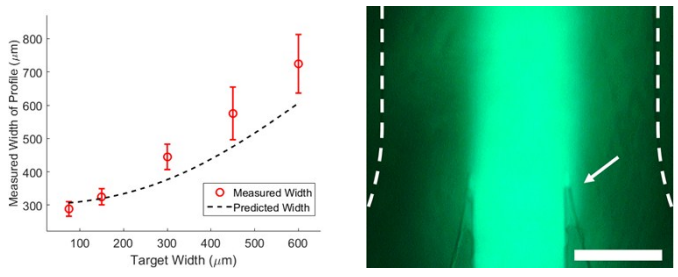

Figure SI-2: Unexpected increased width of concentration profiles. (left) Same data as displayed in Figure 3 with the width predicted by equation 8 plotted as well. Notice that at lower target widths, the theory matches the measurements but for higher target widths, the theory predicts a thinner profile than measured and error bars are wider. (right) Image of a device during a width test. Note that the dye spills over the walls between inlet channels slightly where marked with the arrow. Dotted lines represent the walls of the main channel, scale

which resulted in unsuccessful bonding in the affected regions. While this left most of the chip geometry unaffected, the walls between the inlet channels have clearly not bonded (Figure SI-2 right, white arrow). Close inspection shows that at the junction, these walls do not reach the full height of the channel thus allowing the flow from the central channel to bleed into the side channels before the junction. If this bleed happened uniformly over the whole channel depth there would be no problem, but because some of the designed wall is clearly still present in the device, the bleed cannot be uniform. More specifically, the central stream displaces the side streams more near the PDMS glass interface. This would lead to a non-plug profile if viewed in cross section and would result in an apparent widening of the concentration profile.

For the second potential explanation, consider the time evolution of the width at half max of a diffusing plug. As opposed to a diffusing Gaussian, the width at half max of a diffusing plug first shrinks as the flat high concentration region reduces in width. Thus one interpretation of the data shown in figure SI-2 is that the dye is significantly less diffusive in the direction perpendicular to the flow in the shown experiment when compared to our experiment used to determine the diffusivity of the dye. This may be possible. The experiment used to determine the diffusivity was performed under static conditions whereas the data shown in SI-2 was acquired under flow. Flow can cause the gel to rearrange on a microscopic level and pores can tighten in the direction perpendicular to the flow. As steric hindrance has a significant effect on the diffusivity of large dyes for the gel concentrations used, the diffusivity of the dye may decrease significantly perpendicular to the flow direction leading to the observed wider-than-modeled width at half max.

Taylor Dispersion:

We also considered the potential effects of Taylor dispersion in our system. While this would only affect diffusion in the direction of flow, we felt it important to consider when as it may negatively impact the resolution of the technique during temporal changes in the concentration profile as in the profiles shown in Figure 4.

Here we base our assumption on existing literature [1] where Taylor dispersion in fibrous media is extensively discussed and modeled. They state, with reference to the older work of Durlofsky, [2] that hydrodynamic effects on the diffusivity can be neglected when the volume fraction of the media fall below 5%. In our case we have a 4 mg/mL gel and, assuming that the reported specific volume of collagen of 1.89 ml/g, [3] we come to a volume fraction of 0.76% well below the 5% limit.

References for Taylor Dispersion:

[1] R. J. Phillips, W. M. Deen, and J. F. Brady, *Journal of Colloid and Interfacial Science*, 1990, 139, 363-373

[2] L. Durlofsky, and J. F. Brady, *Physics of Fluids*, 1987, 30, 3329-3341

[3] J.R. Levick, *Quarterly Journal of Experimental Physiology*, 1987, 72, 409-438

Long Term Stability:

To investigate the long term stability of the system, we setup a fixed concentration profile and maintained it for several hours without adjusting the calibration. While these results

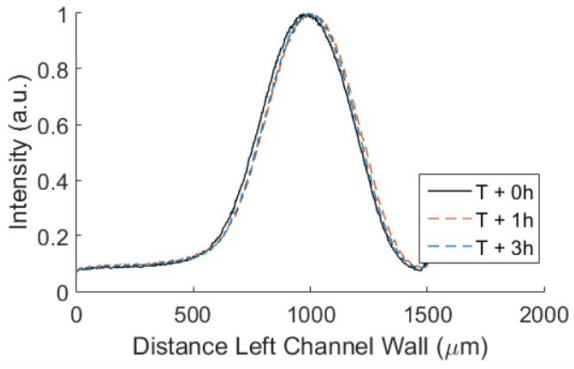

Figure SI-3: Fluorescence intensity profiles from long term stability experiment. Black curve is the initial measurement taken 10 min after flow was started. The red and blue dotted curves show the profiles 1 and 3 hours after the beginning of the experiment respectively.

are preliminary, the results were consistent with the lack of significant deviation during the experiments shown in figure 2 and 3 (these experiments were run in randomized order). The experiments shown in figure SI-3 indicate a drift of 2% in the peak position over the time tested. It is worth noting that that the majority of that drift took place within the first hour and over the next 2 hours the measured drift was 0.3%

Video SI-1:

Video of the time response experiment. Green channel has been subtracted from red channel and contrast enhanced to highlight the faster diffusion of the red dye when compared to the green. At the end of the video, the flow is stopped and the profile allowed to fully diffuse. The video has been sped up slightly. The original capture rate is one frame per 4.25 sec.

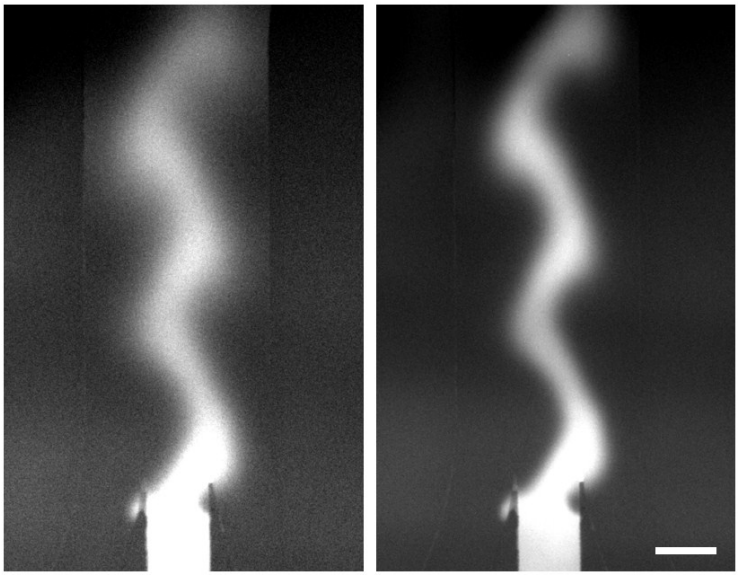

Figure SI-4: Unprocessed red and green channels from the image used to generate Figure 4 in the paper. The red channel is shown on the left while the green channel is shown on the right. Note that the diffusivity of the red dye is still obviously much more diffuse than the green before image processing. To generate the image in the paper, first a threshold was applied to remove the background. Then green image was subtracted from the red. Finally the images were recolored and combined. Scale bar is 500 microns.